Translational Oncology
www.transonc.com

Volume 10 Number 1 February 2017 pp. 17–21 17

Correlations Between DCE MRI and Histopathological Parameters in Head and Neck Squamous Cell Carcinoma[1]

Alexey Surov*, Hans Jonas Meyer†, Matthias Gawlitza*, Anne-Kathrin Höhn‡, Andreas Boehm§, Thomas Kahn* and Patrick Stumpp*

*Department of Diagnostic and Interventional Radiology, University Hospital of Leipzig, Liebigstrasse 20, 04103 Leipzig, Germany; †Department of Radiology, Martin-Luther-University Halle-Wittenberg, Ernst-Grube-Str. 40, 06097 Halle, Germany; ‡Department of Pathology, University Hospital of Leipzig, Liebigstrasse 20, 04103 Leipzig, Germany; §ENT Department, University Hospital of Leipzig, Liebigstrasse 10-14, 04103 Leipzig, Germany

Abstract

BACKGROUND: Dynamic contrast-enhanced magnetic resonance imaging (DCE MRI) can characterize perfusion and vascularization of tissues. DCE MRI parameters can differentiate between malignant and benign lesions and predict tumor grading. The purpose of this study was to correlate DCE MRI findings and various histopathological parameters in head and neck squamous cell carcinoma (HNSCC). *PATIENTS AND METHODS:* Sixteen patients with histologically proven HNSCC (11 cases primary tumors and in 5 patients with local tumor recurrence) were included in the study. DCE imaging was performed in all cases and the following parameters were estimated: K^{trans}, V_e, K_{ep}, and iAUC. The tumor proliferation index was estimated on Ki 67 antigen stained specimens. Microvessel density parameters (stained vessel area, total vessel area, number of vessels, and mean vessel diameter) were estimated on CD31 antigen stained specimens. Spearman's non-parametric rank sum correlation coefficients were calculated between DCE and different histopathological parameters. *RESULTS:* The mean values of DCE perfusion parameters were as follows: K^{trans} 0.189 ± 0.056 min^{-1}, K_{ep} 0.390 ± 0.160 min^{-1}, V_e 0.548 ± 0.119%, and iAUC 22.40 ± 12.57. Significant correlations were observed between K_{ep} and stained vessel areas ($r = 0.51$, $P = .041$) and total vessel areas ($r = 0.5118$, $P = .043$); between V_e and mean vessel diameter ($r = -0.59$, $P = .017$). Cell count had a tendency to correlate with V_e ($r = -0.48$, $P = .058$). In an analysis of the primary HNSCC only, a significant inverse correlation between K^{trans} and KI 67 was identified ($r = -0.62$, $P = .041$). Our analysis showed significant correlations between DCE parameters and histopathological findings in HNSCC.

Translational Oncology (2017) 10, 17–21

Dynamic contrast-enhanced magnetic resonance imaging (DCE MRI) has been reported as a technique which is able to characterize perfusion and vascularization of tissues [1,2]. It has been shown that DCE MRI can be helpful to differentiate between malignant and benign lesions [1]. For example, Yuan et al. reported that lung cancer had a larger volume transfer constant (K^{trans}) and a lower volume of the extravascular extracellular leakage space (V_e) in comparison to benign lesions [3]. Similar results were reported by Li et al. for breast lesions [4]. Furthermore, according to Cho et al., DCE MRI parameters can be used to distinguish prostatic cancer from benign changes [5]. Moreover, DCE MRI parameters can also predict tumor

Address all correspondence to Alexey Surov, Department of Diagnostic and Interventional Radiology, University Hospital of Leipzig, Liebigstrasse 20, 04103 Leipzig, Germany.
E-mail: alex.surow@medizin.uni-halle.de

[1] There was no conflict of extravascular extracellular leakage space interest

Received 10 October 2016; Revised 11 October 2016; Accepted 11 October 2016

1936-5233/17
http://dx.doi.org/10.1016/j.tranon.2016.10.001

grading. As reported previously, K^{trans} correlated well with Gleason score in prostatic cancer [5,6]. According to other reports, K^{trans} and V_e correlated with glioma grade [7,8].

DCE MRI parameters were also associated with prognosis in several malignancies [9,10]. Koo et al. showed that breast cancers with higher K^{trans} or lower V_e had poor prognostic factors and were often of the triple-negative subtype [10].

According to the literature, DCE MRI parameters can predict response to therapy in different tumors. For instance, some authors mentioned that low pretreatment K^{trans} in regional lymph node metastases in head and neck cancer was associated with a poor response to concurrent chemoradiation therapy [11].

Furthermore, Andersen et al. showed that DCE MR parameters obtained prior to chemoradiotherapy predicted survival of patients with cervical cancer [12].

Presumably, DCE MRI parameters may be based on tissue composition, such as cellularity and vascular density. However, in this regard there are contradictory data in the literature. While some studies identified significant correlations between DCE MRI and histopathological parameters, others did not [13–16].

The purpose of this study was to correlate DCE MRI findings and various histopathological parameters in head and neck squamous cell carcinoma (HNSCC).

Material and Methods

This study was IRB-approved and all patients gave their written informed consent.

Patients

Sixteen patients (2 women and 14 men, mean age 57.0 ± 7.5 years, median age 57 years) with histologically proven HNSCC were included in the study. In 11 cases primary HNSCC and in 5 patients local tumor recurrence was diagnosed.

Perfusion Measure

In all cases, dynamic contrast-enhanced (DCE) imaging was performed using T1w DCE sequences according to a protocol reported previously [17]. T1w DCE included 40 subsequent scans à 6 seconds. Imaging parameters were as follows: TR/TE 2.47/0.97 ms, slice thickness 5 mm, flip angle 8°, voxel size 1.2 × 1.0 × 5.0 mm. The contrast application (0.1 mmol Gadobutrol per kg of bodyweight (Gadovist®, Bayer Healthcare, Leverkusen, Germany)) was started after the fifth scan at a rate of 3 ml per second and flushing with 10 ml of normal saline using a power injector (Spectris Solaris, Medrad, Bayer Healthcare, Leverkusen, Germany). The acquired images were transferred to a software module for tissue perfusion estimation (Tissue 4D, Siemens Medical Systems, Erlangen, Germany) as described previously [17,18]. The software offers a population based approach for the arterial input function (AIF) and the best of three available AIF-options was chosen according to the result of the chi2-parameter, which serves as an error measure for the model fit [17]. The AIF was scaled in relation to the gadolinium dose and modeled according to the bi-exponential model of Tofts and Kermode [19].

The following pharmacokinetic parameters were calculated (for exemplary parameter images see Figure 1, *A-E*) [17,18]:

- K^{trans}: volume transfer constant which estimates the diffusion of contrast medium from the plasma through the vessel wall into the interstitial space, representing vessel permeability;
- V_e: volume of the extravascular extracellular leakage space (EES);
- K_{ep}: parameter for diffusion of contrast medium from the EES back to the plasma. It is in close relation with K^{trans} and v_e and is calculated by the formula $k_{ep} = K^{trans} \times V_e^{-1}$;
- iAUC: model-free measurement of the amount of contrast medium delivered to a VOI within a given time period.

In every case, the four parameter maps were projected onto the additionally performed T2 weighted fat-suppressed TSE sequences and the tumor was delineated manually on each slice. This resulted in mean values of K^{trans}, K_{ep}, V_e and iAUC averaged over the complete tumor. Areas of gross necrosis or large feeding vessels were avoided.

Histopathological Analysis

In every case, sections from formalin-fixed and paraffin-embedded tissue were cut at 5 mm and stained with various antigens. The tumor proliferation index was estimated on Ki 67 antigen stained specimens by using MIB-1 monoclonal antibody (DakoCytomation, Denmark) as reported previously [20]. The area with the highest number of positive tumor nuclei was selected for the analysis (Figure 1*F*).

Furthermore, microvessel density was estimated on CD31 antigen stained specimens (DakoCytomation, Denmark) according to the previous description (Figure 1*G*) [21].

All stained samples were digitalized by using a research microscope Jenalumar (Zeiss, Jena, Germany), with camera Diagnostic instruments 4.2., magnification ×400. The digital histopathological images were transferred as uncompressed TIFF images to ImageJ software 1.48v (National Institutes of Health Image program) with a Windows operating system [22,23]. The following histopathological parameters were estimated using the software:

- proliferation index (KI 67) as percentage of stained nuclei;
- cell count as a number of all nuclei;
- stained vessel area (%) calculated as CD 31 positive area divided by the total area of the analyzed histological specimens;
- total vessel area (%), i.e. percentage of vessel area including stained vessel area (CD 31+) and vessel lumen.
- number of vessels;
- mean vessel diameter, i.e. a sum of all stained vessel diameters divided by the number of vessels;

In every case, all histopathological parameters were estimated per two high power fields a 0.16 mm^2.

Statistical Analysis

Statistical analysis and graphics creation was performed with SPSS 20 (IBM SPSS Statistics, Armonk, NY, USA). Values are presented as mean ± SD. Mean value comparison was carried out using the Mann–Whitney *U* test. Spearman's non-parametric rank correlation coefficients were calculated between DCE and different histopathological parameters. Significance level was set at $P \leq .05$.

Results

A complete overview of the results including median values and ranges is shown in Table 1. The mean values of DCE perfusion parameters were as follows: K^{trans} 0.189 ± 0.056 min^{-1}, K_{ep} 0.390 ± 0.160 min^{-1}, V_e 0.548 ± 0.119%, and iAUC 22.40 ± 12.57.

Histopathological analysis yielded the following results: mean cell count was 1033.19 ± 361.67 and the mean level of the proliferation index was 46.25% ± 23.98%. In addition, mean values of tissue vessels were as follows: stained vessel area 6.259% ± 7.831%, total

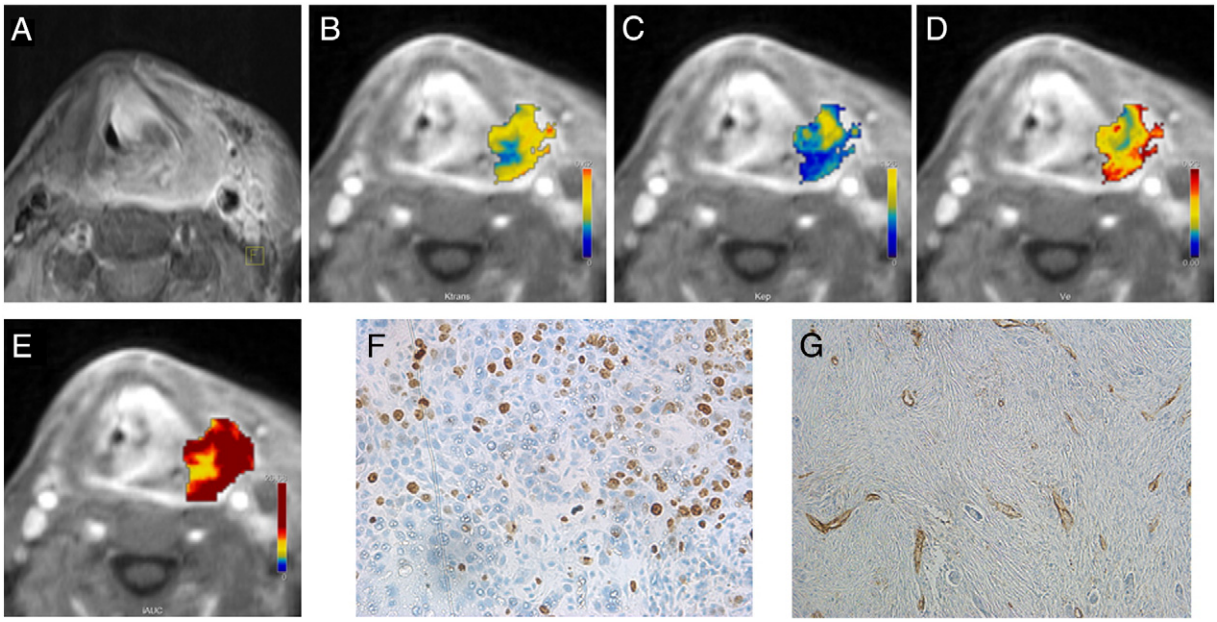

Figure 1. Imaging and histopathological findings in primary hypopharyngeal squamous cell carcinoma. (A) Postcontrast, fat-saturatedT1w image showing a large left-sided cervical mass. (B-E). DCE imaging findings. Estimated DCE parameters are as follows: Ktrans = 0.302 min^{-1} (B), Kep = 0.470 min^{-1} (C), Ve = 0.659% (D), IAUC = 41.77% (E). (F) Immunohistochemical stain (MIB-1 monoclonal antibody). Ki 67 index is 75% and cell count is 789. (G) Immunohistochemical stain (CD 31 monoclonal antibody). Estimated microvessel parameters are as follows: stained vessel area = 0.85%, total vessel area = 1.67%, mean vessel diameter = 15.17 μm, and number of vessels = 28.

Table 1. Analyzed Perfusion and Histopathological Parameters of the Tumors

Parameter	M ± SD	Median	Range
DCE MR parameter			
K^{trans}	0.189 ± 0.056	0.1785	0.079–0.302
K_{ep}	0.390 ± 0.160	0.3605	0.136–0.636
V_e	0.548 ± 0.119	0.5245	0.372–0.743
IAUC	22.40 ± 12.57	25.97	3.028–41.77
Histopathological parameter			
Cell count, n	1033 ± 362	1003	313–1657
Ki 67, %	46.25 ± 23.98	35.00	20–90
Stained vessel area,%	6.259 ± 7.831	2.075	0.77–27.20
Total vessel area, %	7.476 ± 8506	3.687	1.208–30.35
Mean vessel diameter, µm	19.94 ± 7.113	18.34	11.49–35.38
Mean number of vessels, n	53.50 ± 69.41	34.00	15–301

vessel area 7.476% ± 8.506%, mean vessel diameter 19.94% ± 7.113 µm, and mean number of vessels 53.50 ± 69.41 (Table 1).

The results of correlation analysis are shown in Table 2. Significant correlations were observed between K_{ep} and stained vessel areas (r = 0.51, P = .041) and total vessel areas (r = 0.5118, P = .043); between V_e and mean vessel diameter (r = –0.59, P = .017). Cell count had a tendency to correlate with V_e (r = –0.48, P = .058).

There were no significant correlations between other analyzed parameters (Table 2).

In an analysis of the primary HNSCC only, a significant inverse correlation between K^{trans} and KI 67 was identified (r = –0.62, P = .041). Furthermore, stronger significant correlations were found between K_{ep} and stained vessel areas, total vessel areas, and between V_e and mean vessel diameter (Table 3).

Discussion

The present study documents significant correlations between different DCE MRI and histopathological parameters in HNSCC.

Previously, some studies also analyzed relationships between histological and perfusion parameters in several malignancies. For instance, Li et al. showed that the mean K^{trans} and K_{ep} values significantly correlated with microvessel density in breast cancer [4]. According to Oto et al. K_{ep} positively correlated with the mean blood vessel count and mean vessel area fraction parameters calculated by CD31 staining in prostate cancer [13]. Additionally, the mean blood vessel count and mean vessel area fraction parameters showed a moderate negative correlation with V_e [13].

However, according to the literature several tumors had different associations between DCE and histopathological parameters. For

Table 2. Identified Correlations Between DCE Perfusion and Histopathological Parameters in HNSCC

Parameters	$K^{trans-1}$, min	K_{ep}^{-1}, min	V_e, %	IAUC
Cell count, n	r = –0.12 (P = .65)	r = 0.17 (P = .53)	r = –0.48 (P = .058)	r = –0.24 (P = .38)
Ki 67, %	r = –0.16 (P = .56)	r = –0,13 (P = .63)	r = –0,061 (P = .82)	r = –0,15 (P = .58)
Stained vessel area, %	r = 0.21 (P = .42)	r = 0.51 (P = .041)	r = –0.38 (P = .14)	r = 0,4147 (P = .11)
Total vessel area, %	r = 0.24 (P = .38)	r = 0.51 (P = .043)	r = –0.39 (P = .13)	r = 0.32 (P = .22)
Mean vessel diameter, µm	r = 0.021 (P = .94)	r = 0.39 (P = .13)	r = –0,59 (P = .017)	r = –0.026 (P = .92)
Mean number of vessels, n	r = 0.23 (P = .39)	r = 0.14 (P = .61)	r = 0.031 (P = .91)	r = 0.22 (P = .42)

Table 3. Identified Correlations Between DCE Perfusion and Histopathological Parameters in Primary HNSCC (n = 11)

Parameters	$K^{trans-1}_{,\ min}$	$K^{-1}_{ep,\ min}$	$V_{e,\ \%}$	IAUC
Cell count, n	r = −0.25 (P = .47)	r = 0.0001 (P = .99)	r = −0.37 (P = .27)	r = −0.29 (P = .37)
Ki 67, %	r = −0.62 (P = .041)	r = −0.45 (P = .16)	r = −0.16 (P = .64)	r = −0.49 (P = .129)
Stained vessel area, %	r = 0.21 (P = .53)	r = 0.67 (P = .02)	r = −0.53 (P = .096)	r = 0.31 (P = .34)
Total vessel area, %	r = 0.07 (P = .83)	r = 0.62 (P = .04)	r = −0.65 (P = .03)	r = 0.29 (P = .38)
Mean vessel diameter, µm	r = −0.17 (P = .62)	r = 0.43 (P = .18)	r = −0.69 (P = .017)	r = 0.06 (P = .85)
Mean number of vessels, n	r = 0.24 (P = .49)	r = 0.23 (P = .49)	r = −0.048 (P = .88)	r = 0.32 (P = .32)

example, Jia et al. found that K^{trans} and V_e were both positively correlated with microvessel density in high grade glioma, but not in low grade tumors [14].

Our results confirmed these findings. We also found statistically significant positive correlations between K_{ep} and vessel areas in our cases. Furthermore, V_e correlated inversely with mean vessel diameter. Moreover, these correlations were stronger in primary tumors.

As reported previously, DCE parameters correlated not only with vessel density, but also with other tumor markers in different malignancies. For instance, Aryal et al. reported that V_e significantly correlated with tumor cellularity in glioma [15]. Jansen et al. identified a significant correlation between K_{ep} and expression level of vascular endothelial growth factor in cervical lymph node metastases from HNSCC [16]. The authors also found that KI 67 inversely correlated with K^{trans} and V_e [16].

In the present study, we found no significant correlations between cell count or KI 67 and DCE MRI parameters. Only V_e tended to correlate with cell count.

However, in the cases with primary tumors K^{trans} correlated significantly inversely with KI 67. This fact suggests different associations between DCE parameters and histopathology in primary versus recurrent tumors.

Similar relationships were reported previously in other malignancies. For instance, perfusions parameters correlated well with KI 67 in glioma, when the data from high and low grade tumors were combined [24]. However, no significant correlation was observed in high or low grade tumors, when they were analyzed separately [24].

The associations between DCE MRI and histopathological parameters identified in the present analysis may be helpful to differentiate HNSCC with low and high proliferation potential. Similarly, the use of DCE MRI can also distinguish tumors with high angiogenesis from lesions with low microvessel density. Therefore, DCE MRI parameters can be used as a noninvasive tool for tumor angiogenesis. In fact, according to Song et al., K^{trans} and V_e values decreased statistically significantly after anti-angiogenic treatment in an orthotopic mouse model of human hepatocellular carcinoma [25]. Other authors confirmed these results [26]. This leads to the assumption that DCE MRI may predict response to anti-angiogenic therapy. Presumably, tumors with high microvessel density have a better response to anti-angiogenic drugs.

Clearly, further works with more cases are needed to confirm our results and to search for other relevant relationships between DCE and histopathology in different malignancies.

In conclusion, our analysis showed significant correlations between K_{ep}, V_e and microvessel density in HNSCC. V_e also tended to correlate with cell count.

In primary tumors, the correlations between K_{ep}, V_e and vessel parameters were stronger. Furthermore, in primary tumors, K^{trans} correlated significantly with KI 67.

References

[1] Bernstein JM, Homer JJ, and West CM (2014). Dynamic contrast-enhanced magnetic resonance imaging biomarkers in head and neck cancer: potential to guide treatment? A systematic review. *Oral Oncol* **50**, 963–970.

[2] van Niekerk CG, van der Laak JA, Hambrock T, Huisman HJ, Witjes JA, Barentsz JO, and Hulsbergen-van de Kaa CA (2014). Correlation between dynamic contrast-enhanced MRI and quantitative histopathologic microvascular parameters in organ-confined prostate cancer. *Eur Radiol* **24**, 2597–2605.

[3] Yuan A, Lin CY, Chou CH, Shih CM, Chen CY, Cheng HW, Chen YF, Chen JJ, Chen JH, and Yang PC, et al (2011). Functional and structural characteristics of tumor angiogenesis in lung cancers overexpressing different VEGF isoforms assessed by DCE- and SSCE-MRI. *PLoS One* **6**, e16062.

[4] Li L, Wang K, Sun X, Wang K, Sun Y, Zhang G, and Shen B (2015). Parameters of dynamic contrast-enhanced MRI as imaging markers for angiogenesis and proliferation in human breast cancer. *Med Sci Monit* **21**, 376–382.

[5] Cho E, Chung DJ, Yeo DM, Sohn D, Son Y, Kim T, and Hahn ST (2015). Optimal cut-off value of perfusion parameters for diagnosing prostate cancer and for assessing aggressiveness associated with Gleason score. *Clin Imaging* **39**, 834–840.

[6] Puech P, Potiron E, Lemaitre L, Leroy X, Haber GP, Crouzet S, Kamoi K, and Villers A (2009). Dynamic contrast-enhanced-magnetic resonance imaging evaluation of intraprostatic prostate cancer: correlation with radical prostatectomy specimens. *Urology* **74**, 1094–1099.

[7] Choi HS, Kim AH, Ahn SS, Shin NY, Kim J, and Lee SK (2013). Glioma grading capability: comparisons among parameters from dynamic contrast-enhanced MRI and ADC value on DWI. *Korean J Radiol* **14**, 487–492.

[8] Li X, Zhu Y, Kang H, Zhang Y, Liang H, Wang S, and Zhang W (2015). Glioma grading by microvascular permeability parameters derived from dynamic contrast-enhanced MRI and intratumoral susceptibility signal on susceptibility weighted imaging. *Cancer Imaging* **15**, 4.

[9] Ng SH, Lin CY, Chan SC, Yen TC, Liao CT, Chang JT, Ko SF, Wang HM, Huang SF, and Lin YC, et al (2013). Dynamic contrast-enhanced MR imaging predicts local control in oropharyngeal or hypopharyngeal squamous cell carcinoma treated with chemoradiotherapy. *PLoS One* **8**(8), e72230.

[10] Koo HR, Cho N, Song IC, Kim H, Chang JM, Yi A, Yun BL, and Moon WK (2012). Correlation of perfusion parameters on dynamic contrast-enhanced MRI with prognostic factors and subtypes of breast cancers. *J Magn Reson Imaging* **36**, 145–151.

[11] Kim S, Loevner LA, Quon H, Kilger A, Sherman E, Weinstein G, Chalian A, and Poptani H (2010). Prediction of response to chemoradiation therapy in squamous cell carcinomas of the head and neck using dynamic contrast-enhanced MR imaging. *AJNR Am J Neuroradiol* **31**, 262–268.

[12] Andersen EK, Hole KH, Lund KV, Sundfør K, Kristensen GB, Lyng H, and Malinen E (2013). Pharmacokinetic parameters derived from dynamic contrast enhanced MRI of cervical cancers predict chemoradiotherapy outcome. *Radiother Oncol* **107**, 117–122.

[13] Oto A, Yang C, Kayhan A, Tretiakova M, Antic T, Schmid-Tannwald C, Eggener S, Karczmar GS, and Stadler WM (2011). Diffusion-weighted and dynamic contrast-enhanced MRI of prostate cancer: correlation of quantitative MR parameters with Gleason score and tumor angiogenesis. *AJR Am J Roentgenol* **197**, 1382–1390.

[14] Jia ZZ, Gu HM, Zhou XJ, Shi JL, Li MD, Zhou GF, and Wu XH (2015). The assessment of immature microvascular density in brain gliomas with dynamic contrast-enhanced magnetic resonance imaging. *Eur J Radiol* **84**, 1805–1809.

[15] Aryal MP, Nagaraja TN, Keenan KA, Bagher-Ebadian H, Panda S, Brown SL, Cabral G, Fenstermacher JD, and Ewing JR (2014). Dynamic contrast enhanced MRI parameters and tumor cellularity in a rat model of cerebral glioma at 7 T. *Magn Reson Med* **71**, 2206–2214.

[16] Jansen JF, Carlson DL, Lu Y, Stambuk HE, Moreira AL, Singh B, Patel SG, Kraus DH, Wong RJ, and Shaha AR, et al (2012). Correlation of a priori

DCE-MRI and (1)H-MRS data with molecular markers in neck nodal metastases: Initial analysis. *Oral Oncol* **48**, 717–722.

[17] Gawlitza M, Purz S, Kubiessa K, Boehm A, Barthel H, Kluge R, Kahn T, Sabri O, and Stumpp P (2015). In vivo correlation of glucose metabolism, cell density and microcirculatory parameters in patients with head and neck cancer: Initial results using simultaneous PET/MRI. *PLoS One* **10**, e0134749.

[18] Bisdas S, Seitz O, Middendorp M, Chambron-Pinho N, Bisdas T, Vogl TJ, Hammerstingl R, Ernemann U, and Mack MG (2010). An exploratory pilot study into the association between microcirculatory parameters derived by MRI-based pharmacokinetic analysis and glucose utilization estimated by PET-CT imaging in head and neck cancer. *Eur Radiol* **20**, 2358–2366.

[19] Tofts PS and Kermode AG (1991). Measurement of the blood–brain barrier permeability and leakage space using dynamic MR imaging. 1. Fundamental concepts. *Magn Reson Med* **17**, 357–367.

[20] Roser F, Samii M, Ostertag H, and Bellinzona M (2004). The Ki-67 proliferation antigen in meningiomas. Experience in 600 cases. *Acta Neurochir* **146**, 37–44.

[21] Weidner N, Semple JP, Welch WR, and Folkman J (1991). Tumor angiogenis and metastasis: correlation in invasive breast carcinoma. *N Engl J Med* **324**, 1875–1887.

[22] Aoyagi T, Shuto K, Okazumi S, Hayano K, Satoh A, Saitoh H, Shimada H, Nabeya Y, Kazama T, and Matsubara H (2012). Apparent diffusion coefficient correlation with oesophageal tumour stroma and angiogenesis. *Eur Radiol* **22**, 1172–1777.

[23] Surov A, Caysa H, Wienke A, Spielmann RP, and Fiedler E (2015). Correlation between different ADC fractions, cell count, Ki-67, total nucleic areas and average nucleic areas in meningothelial meningiomas. *Anticancer Res* **35**, 6841–6846.

[24] Jain KK, Sahoo P, Tyagi R, Mehta A, Patir R, Vaishya S, Prakash N, Vasudev N, and Gupta RK (2015). Prospective glioma grading using single-dose dynamic contrast-enhanced perfusion MRI. *Clin Radiol* **70**, 1128–1135.

[25] Song KD, Choi D, Lee JH, Im GH, Yang J, Kim JH, and Lee WJ (2014). Evaluation of tumor microvascular response to brivanib by dynamic contrast-enhanced 7-T MRI in an orthotopic xenograft model of hepatocellular carcinoma. *AJR Am J Roentgenol* **202**, W559–W566.

[26] Noij DP, de Jong MC, Mulders LG, Marcus JT, de Bree R, Lavini C, de Graaf P, and Castelijns JA (2015). Contrast-enhanced perfusion magnetic resonance imaging for head and neck squamous cell carcinoma: a systematic review. *Oral Oncol* **51**, 124–138.